Plant Physiol. (1997) 113: 387–395

Polyamines and Pectins

I. Ion Exchange and Selectivity

Johan Messiaen, Pierre Cambier, and Pierre Van Cutsem*

Facultés Universitaires Notre-Dame de la Paix, Laboratoire de Biotechnologie Théorique, 61 Rue de Bruxelles, B-5000 Namur, Belgium

The ion-binding and -exchange properties of putrescine, spermidine, and spermine on purified walls of carrot (*Daucus carota* L.) cell suspensions were investigated by producing ion-exchange isotherms and comparing them with the behavior of Na^+, Mg^{2+}, and Ca^{2+}. The cation exchange capacity of the carrot cell walls was 0.8 equivalent kg^{-1} dry matter, and the ionic selectivity sequence of the walls for polyamines followed the sequence spermine^{4+} > spermidine^{3+} ≈ Ca^{2+} > putrescine^{2+}. The polyamines were subjected to only electroselectivity and probably did not induce any favorable supramolecular conformation of pectin like the one induced by Ca^{2+}. Triangular ion exchanges were also performed with three diamines: ethanediamine, butanediamine, and octanediamine. The shorter the diamine, the higher the total adsorption and selectivity of the exchange. The lower selectivity of the cell wall for putrescine was partly attributed to its inability to access and displace Ca^{2+} from higher affinity sites within dimerized pectic sequences. The polyamine adsorption and exchange on pectic sequences could result in pectic signal modulation in pathogenesis and in differentiation.

PAs are ubiquitous polycationic molecules found in almost every cell compartment, including the cell wall. They are deeply involved in a whole series of cellular events concerned with growth and differentiation, including germination, organ formation, flowering, and senescence, and many of these effects depend on cell division (Egea-Cortines and Mizrahi, 1991).

One of the most studied effects of PAs on plant cells is their involvement in embryogenesis in carrot (*Daucus carota* L.) cells (Montague et al., 1979; Bastola and Minocha, 1995). The deletion of 2,4-D from the growth medium of carrot cells has a permissive effect on somatic embryogenesis, correlated with a Put^{2+} increase within 24 h of the removal of the growth regulator. The transfer and expression of a mouse Orn decarboxylase cDNA increases the cellular concentration of Put^{2+} and increases the efficiency of somatic embryogenesis in the absence or presence of 2,4-D (Bastola and Minocha, 1995). Even in this well-known system of carrot embryogenesis, most of the available literature is essentially concerned with dose-response relationships; the molecular mechanisms of PA action are still not clear.

The polycationic nature of PAs at physiological pH is one of the main properties believed to mediate their biological activity. PAs are indeed able to bind several negatively charged molecules such as DNA (Basu et al., 1990), proteins (Apelbaum et al., 1988), membrane phospholipids and proteins (Schuber et al., 1983; Tassoni et al., 1996), and pectic polysaccharides (D'Orazi and Bagni, 1987). They are involved in protein phosphorylation (Ye et al., 1994), post-transcriptional modifications (Mehta et al., 1994), and conformational transition of DNA (Basu et al., 1990).

The role of PAs in the cell wall, however, has not to our knowledge been elucidated. Endogenous pectin-associated PAs are present in small amounts (10–50 μmol kg^{-1} fresh weight in suspension-cultured carrot cells, Mariani et al., 1989). These concentrations vary depending on the stage of development, the pH, and the Ca^{2+} content of the cell wall, and on the presence of DA- and PA-degrading enzymes (Mariani et al., 1989; Angelini et al., 1993).

It has been proposed that PAs could be part of an intrinsic signaling network of the extracellular matrix. D'Orazi and Bagni (1987) showed that Put^{2+}, Spd^{3+}, and Spm^{4+} were able to bind pectin in solution, thereby decreasing the pH. They postulated that pectin-associated PAs are one of many factors that might regulate cell wall expansion by changing the cell wall pH. Moustacas et al. (1991) and Charnay et al. (1992) proposed that the formation of pectin-PA complexes in the cell wall would facilitate the recognition of pectin by pectin methylesterases. PAs would also be part of a set of cell wall modulators involved in host-pathogen interactions. Angelini et al. (1993) showed that DA and PA oxidase activities are indeed tightly coupled to cell wall peroxidase activity. The degradation of PAs might therefore be involved in the release of hydrogen peroxide and in the lignification of the cell wall.

Pectin-bound PAs are thus involved in many physiological processes affecting directly the shape, function, and/or survival of the cell. However, the way PAs and pectic substances interact physicochemically has not to our knowledge been characterized. Before trying to physiologically relate PAs to pectic polysaccharides, it is therefore essential to have a better physicochemical understanding

* Corresponding author; e-mail pierre.vancutsem@fundp.ac.be; fax 32–81–724420.

Abbreviations: CEC, cationic exchange capacity; DA, diamine; DE, diaminoethane; DO, diamino-octane; PA, polyamine; PGA, homopolygalacturonic acid; Put^{2+}, putrescine; Spd^{3+}, spermidine; Spm^{4+}, spermine.

of their molecular interactions within the extracellular matrix. We therefore undertook a systematic study of the interactions between PAs and cell walls.

In this paper, we describe the binding and exchange properties of three PAs (Put^{2+}, Spd^{3+}, and Spm^{4+}) and two DAs (octanediamine and ethanediamine) to isolated walls of carrot suspension cells. We also report the competition between PAs and protons and compare it with the adsorption of the inorganic cations Na^+, Mg^{2+}, and Ca^{2+}.

MATERIALS AND METHODS

Carrot Cell Suspension and Cell Wall Isolation

Carrot (*Daucus carota* L.) cells were maintained in supplemented Murashige-Skoog medium (Murashige and Skoog, 1962) containing 4.708 g L^{-1} Murashige-Skoog salts, 1 mg L^{-1} 2,4-D, and 30 g L^{-1} Suc (pH 5.7). Cells were grown in 50 mL of supplemented Murashige-Skoog medium in 250-mL flasks under constant agitation (110 rpm) on an Edmund Bühler orbital rotator (model VKS 75, Van Hopplynus, Brussels, Belgium) at 25°C in the dark. Cells were subcultured every 15 d using a 1:4 dilution.

Cell walls were obtained from 1 L of a 6-d-old cell suspension. Cells were filtered through Miracloth (Calbiochem) and washed several times with deionized water before being resuspended in 100 mL of deionized water. Cells were pressurized in a cell disruption bomb (model 4639 Parr, Analis, Namur, Belgium) for 15 min at 7 MPa and exploded by a rapid depressurization. The disrupted cells were pelleted by centrifugation at 3000*g* for 15 min at 4°C. Cell walls were washed successively in ether, dichloromethane, and acetone to remove membrane phospholipids and cytosolic debris (York et al., 1985). Washed cell walls were finally resuspended in 100 mL of deionized water containing 0.1% (w/v) sodium azide and stored at 4°C until use.

Ca^{2+}-PA and PA-PA Ion Exchange

Five-hundred microliters of a carrot cell wall preparation (approximately 1.8 mg fresh weight) was used for each point in the isotherms. Cell walls were equilibrated at room temperature in 10 mN mixtures of $CaCl_2$-Put^{2+}, $CaCl_2$-ethanediamine, $CaCl_2$-octanediamine, $CaCl_2$-Spd^{3+}, $CaCl_2$-Spm^{4+}, Put^{2+}-Spd^{3+}, Put^{2+}-Spm^{4+}, or Spd^{3+}-Spm^{4+}, with various equivalent fractions at a pH of approximately 5.7. The treatment solutions (approximately 10 mL) were renewed five times (once every hour). The cell walls were then pelleted by centrifugation at 13,000*g* for 15 min at room temperature and the supernatant was discarded.

Proton-Cation Exchanges

Five-hundred microliters of a carrot cell wall preparation (approximately 1.8 mg fresh weight) was also used for each treatment. Cell walls were equilibrated at room temperature with approximately 10 mL of 0.1 or 10 mN Put^{2+}, ethanediamine, octanediamine, Spd^{3+}, Spm^{4+}, Na^+, Mg^{2+}, and Ca^{2+} solutions at pH values adjusted between 5.7 and 1.0 by the addition of HCl. The treatment solutions were renewed five times (once every hour). Cell walls were recovered by centrifugation at 13,000*g* for 15 min at room temperature. The supernatant was collected and the equilibrium pH measured immediately using a pH electrode (LIQ-PLAST P/N:238'010, Hamilton Filter Service, Eupea, Belgium) connected to a pH meter (model P614, Consort, Turnhout, Belgium). The pelleted cell walls were further dried for 48 h at 50°C and weighed using an electrobalance (model 708501, Sartorius, Van der Heyden, Brussels, Belgium).

Extraction and Analysis of Cations

Inorganic cations and PAs were extracted from the pelleted cell walls by overnight incubation in 0.5 mL of 5% (w/v) $HClO_4$, pH approximately 0.6, at 4°C with mild agitation.

The Na^+, Mg^{2+}, Ca^{2+}, and Cu^{2+} contents of the treated cell walls were determined in 0.4 mL of the 5% $HClO_4$ extract using a atomic absorption spectrophotometer (model PU 9200X, Pye-Unicam, Cambridge, UK).

Analysis of PA

The PA content of the treated cell walls was determined in 0.1 mL of the 5% (w/v) $HClO_4$ extract in the presence of 50 μL of 0.845 mN diaminoheptane (internal standard), 400 μL of dansyl chloride (30 mg mL^{-1} dissolved in acetone), and 200 μL of saturated Na_2CO_3. The samples were vortexed and incubated at 60°C for 60 min in the dark. Excess dansyl chloride was removed by adding 100 μL of Pro (100 mg mL^{-1}) and by incubating the samples for a further 60 min at room temperature in the dark. Dansylated PAs were extracted with 500 μL of toluene, vortexed, and centrifuged at 5000*g* for 5 min at room temperature. The upper organic phase was collected and dried under N_2. The dry residue was finally resuspended in 500 μL of acetonitrile just before HPLC analysis.

PAs were analyzed by HPLC. Thirty microliters of each sample was injected with an auto-injector (model Sil-10A, Shimadzu Scientific Instruments, Columbia, MD) on a high-resolution Rsil C_{18} HL column equilibrated in 72% (v/v) acetonitrile. The separated PAs were detected using a scanning fluorescence detector (model 470, Waters; excitation wavelength = 320 nm; emission wavelength = 510 nm) connected to an integrator (model CR4A Chromatopac, Shimadzu). To take into account the PA-specific sensitivity of the fluorescence detector, the PA-to-diaminoheptane peak surface ratio was compared with calibration curves established for each PA, with diaminoheptane as the internal standard.

CEC Determination

Carrot cells (approximately 1.8 mg) were equilibrated in 10 mN $CuCl_2$ (pH approximately 5.7) solutions as for the previous cationic exchanges. Cell walls were rinsed in 10 mL of H_2O and recovered by centrifugation at 13,000*g* for 15 min at room temperature. The supernatant was discarded and the cell walls were dried at 50°C for 48 h. The

cell walls were then weighed and Cu^{2+} was extracted overnight at 4°C under mild agitation with 1 mL of 1 N HCl containing 1 mg mL^{-1} CsCl. Cell wall Cu^{2+} content was assayed by atomic absorption spectrophotometry. The total cation exchange capacity was expressed as equivalents kg^{-1} dry weight.

Ion-Exchange Isotherms

Ion-exchange isotherms between cations were calculated according to the method of Van Cutsem and Gillet (1981). A cation-exchange reaction between two ions, A and B, on 1 equivalent of ion exchanger may be stated as follows:

$$\frac{\bar{A}}{z_a} + \frac{B}{z_b} \Leftrightarrow \frac{\bar{B}}{z_b} + \frac{A}{z_a}$$

The bar denotes the ion in the adsorbed phase, and z_a and z_b are the valencies of the cations. From the composition of the exchanger and the solution phases, the empirical selectivity coefficient on equivalent fraction basis, K_N, can be deduced:

$$K_N = \frac{(\overline{N_b})^{1/z_b}(a_a)^{1/z_a}}{(\overline{N_a})^{1/z_a}(a_b)^{1/z_b}}$$

where $\overline{N_a}$ and $\overline{N_b}$ are the equivalent fractions of ion species A and B in the adsorbed phase, and a_a and a_b are the solution phase activities.

Molecular Distances

The compounds were generated with the builder module of the InsightII 95.0 program (Biosym Technologies, San Diego, CA) using default fragments (amine, butyl, and propyl groups). The molecules were fixed in their protonated state (sp^3 hybridization for the N atoms, similar to the one of a C in a saturated chain). Both C—N—C and C—C—C bond angles thus tend to 109°.

All geometries were optimized by a three-step (Steepest Descent, Conjugate Gradient, Newton-Raphson) molecular mechanics process using the cff91 forcefield (Maple et al., 1984, 1988) with the Discover program (Biosym). The visualization of the minimized geometries and the measurement of the inter-N distances were performed on an IBM RS-6000 computer.

RESULTS AND DISCUSSION

The aim of this work was to study the behavior of PAs in the cell wall matrix and to see how PAs interact with pectins. We therefore compared the ion-exchange properties of PAs in *D. carota* cell walls with those of major cations such as Na^+, Mg^{2+}, and Ca^{2+}. Since plant cells excrete large amounts of protons, we also investigated the cation-proton exchanges.

CEC of the Cell Walls

The CEC of isolated cell walls from cell suspensions of carrot was measured for a series of cations, including PAs and mono- and bivalent mineral cations. The CEC measured with Ca^{2+} or Cu^{2+} (or Spd^{3+} or Spm^{4+}) amounts to about 0.8 equivalent kg^{-1} dry matter (Fig. 1). The wall CEC for Spd^{3+} and Spm^{4+} was nearly identical to the one for Cu^{2+}, despite the fact that Spd^{3+} and Spm^{4+} were not able to displace a small, residual amount (approximately 5% of the CEC) of Ca^{2+}, even in the presence of 100% 10 mN PAs in the bathing solutions.

The maximum amount of Put^{2+} adsorbed at a pH of approximately 5.7 was approximately 0.6 equivalent kg^{-1} dry matter, i.e. only three-quarters of the maximum CEC. The behavior of Put^{2+} is therefore somewhat similar to that of Mg^{2+}. Although bivalent, this last cation saturates about 85 and 76% of the uronic sites of the cell walls of *D. carota* and *Nitella flexilis*, respectively, (P. Van Cutsem, unpublished result). Its large hydration sphere increases its minimum distance of approach, preventing it from interacting electrostatically as strongly as Ca^{2+} with the carboxylates (Fig. 1).

Exchange between Inorganic Cations and Protons

The exchange of monovalent and bivalent cations for protons on carrot cell walls conformed to previous observations on other plant systems with a selectivity sequence of $Ca^{2+} > Mg^{2+} \approx Na^+$ (Fig. 2). The selectivity sequence can be partly explained by the electroselectivity that favors the adsorption of divalent over monovalent cations and by the larger hydration of Mg^{2+} ions, as discussed above.

Ca^{2+}-PA Exchange Isotherms

The binding and exchange properties of Put^{2+}, Spd^{3+}, and Spm^{4+} to cell wall pectins were studied in the presence of Ca^{2+}. Wall samples were equilibrated at a pH of approximately 5.7 in solutions of varying proportions of PAs and Ca^{2+} at 10 mN total concentrations. The amounts of Put^{2+}, Spd^{3+}, and Spm^{4+} adsorbed in the cell walls ($\bar{N}_{PA}$, equivalent fraction of the adsorbed PA) were expressed as a function of the free Put^{2+}, Spd^{3+}, and Spm^{4+} in the equilibrium solutions (X_{PA}, equivalent fraction of the PA in solution), respectively.

In the Ca^{2+}-Put^{2+} exchange isotherm (Fig. 3A), the cell walls exhibited a preference for Put^{2+} over the first 20 to 30% of the exchange isotherm, and for Ca^{2+} over the rest of

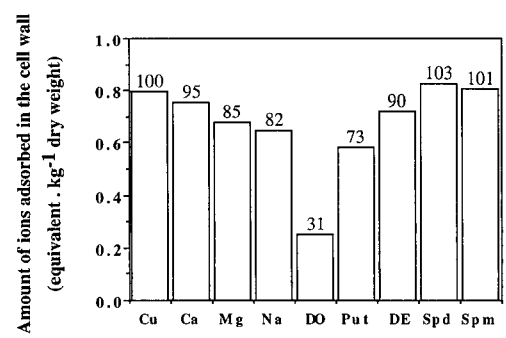

Figure 1. CEC of carrot cells for inorganic cations, DAs, and PAs. The number above each column represents the percentage of the total CEC accessible to the cation.

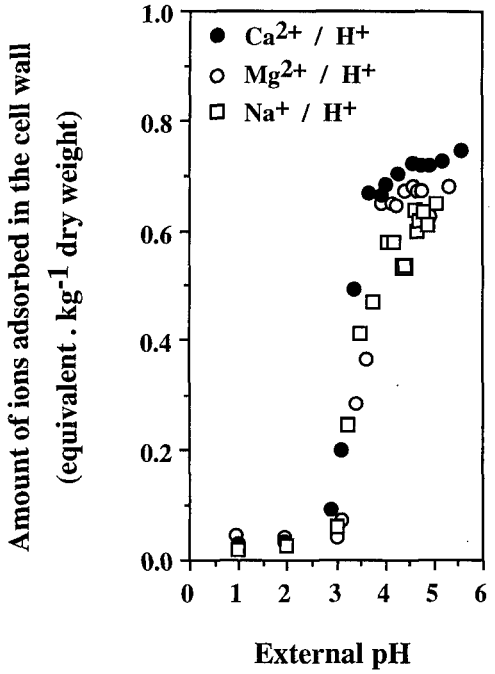

Figure 2. Effect of the external pH on the amount of Ca^{2+}, Mg^{2+}, and Na^{+} adsorbed in carrot cell walls in equilibrium with 10 mN ionic solutions.

the exchange sites; this is reflected by a negative value of the selectivity coefficient K_N on a logarithmic scale (Fig. 3B). However, the selectivity of the wall for Ca^{2+} at the expense of Put^{2+} is somewhat biased by the fact that the CEC for Put^{2+} is only 0.59 equivalent kg^{-1}, i.e. approximately three-quarters of the total CEC. The unoccupied sites are compensated for by protons, as will be confirmed by the PA-proton adsorption isotherms. It is not clear at this point whether this weaker interaction of Put^{2+} was caused by a different hydration of the organic cation or by charge density and steric considerations due to charge distribution over N atoms separated from each other by four C atoms.

The selectivity coefficient K_N of the cell wall toward Put^{2+} was not constant: it decreased quickly and continuously as its content in the cell walls increased. A selectivity reversal was observed at Put^{2+} contents of 25%, clearly indicating that the exchange sites for the adsorption of Put^{2+} and Ca^{2+} are heterogeneous.

The Spd^{3+}-Ca^{2+} exchange isotherm was close to the diagonal, reflecting the absence of clear selectivity for any of the competing cations. The logarithm of the selectivity coefficient K_N was indeed very close to 0 when less than 70% of the exchange sites were occupied by Spd^{3+}. The last 30% of the CEC bound Ca^{2+} more strongly, which is reflected by the negative values of the apparent pK at high coverage of the exchanger. This absence of selectivity of Spd^{3+} is surprising considering the higher valence of the PA.

In the Spm^{4+}-Ca^{2+} exchange isotherm, the carrot cell walls adsorbed the tetravalent Spm^{4+} more selectively. The natural logarithm of the selectivity coefficient K_N for Spm^{4+} was thus positive for about 80% of the exchange, the last 20% of the uronates showing a clear selectivity toward Ca^{2+}.

PA-PA Exchange Isotherms

Ion-exchange isotherms between the PAs themselves were also performed. Carrot cell walls were equilibrated in Put^{2+}-Spd^{3+}, Put^{2+}-Spm^{4+}, and Spd^{3+}-Spm^{4+} solutions in the absence of Ca^{2+} in the treatment solutions. The cell walls exhibited a net preference for the higher charged polycations, defining the following selectivity sequence: $Spm^{4+} > Spd^{3+} > Put^{2+}$ (Fig. 4A). The natural logarithm of the selectivity coefficient for each isotherm was therefore positive when expressed against the preferred adsorbed PA in the carrot cell walls (Fig. 4B). It was interesting that the selectivity of the wall for Spd^{3+} versus Put^{2+} was significantly stronger than the selectivity of Spm^{4+} versus Spd^{3+}: the effect of one additional charge is proportionally higher in the case of the Spd^{3+} versus Put^{2+} isotherm, but most importantly, Put^{2+} cannot access one-quarter of the exchange sites.

PA-H^+ Exchange

The effect of cell wall pH on PA adsorption was studied. Carrot cell walls were equilibrated in 0.1 and 10 mN pure

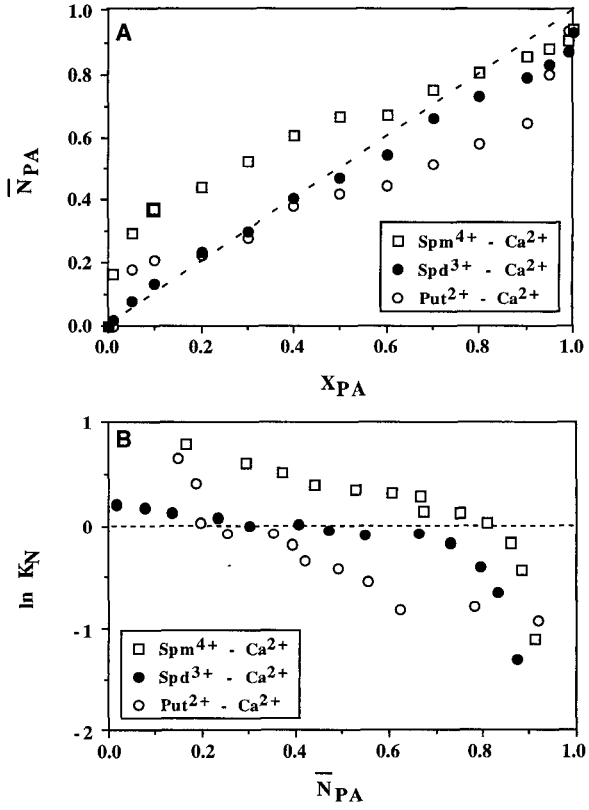

Figure 3. PA-Ca^{2+} ion-exchange isotherms. A, Equivalent fraction of PAs adsorbed in the carrot cell wall ($\bar{N}_{PA}$) versus the equivalent fraction of PAs ($\bar{N}_{PA}$) present in the bathing solutions. B, Natural logarithm of the selectivity coefficient K_N of the exchanges versus the equivalent fraction of PAs adsorbed in the cell wall ($\bar{N}_{PA}$). For the clarity of the graph, Put^{2+} is considered here as a PA.

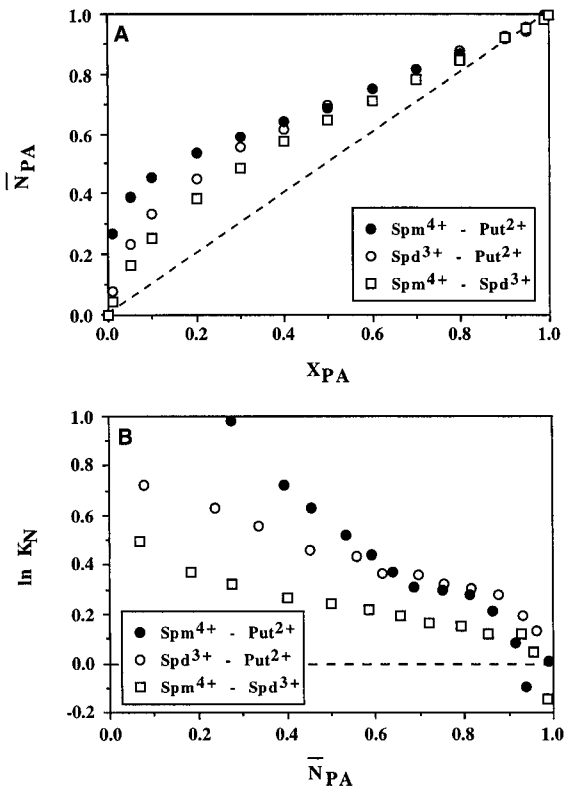

Figure 4. PA-PA ionic exchange isotherm. A, Equivalent fraction of the preferred PAs (Spm^{4+}, Spd^{3+}, and Spm^{4+}) adsorbed in the carrot cell walls ($\overline{N}_{PA}$) versus the equivalent fraction of the same PAs (X_{PA}) present in the bathing solutions. B, Natural logarithm of the selectivity coefficients K_N versus the equivalent fractions of the preferred PAs adsorbed in the cell wall ($\overline{N}_{PA}$). For the clarity of the graph, Put^{2+} is considered here as a PA.

PA solutions at different pHs in the absence of competing Ca^{2+} in the bathing solutions. The amount of PA adsorbed in the cell walls was determined for a range of pH values between 1 and 6. Above pH 3.5, the amount of PAs bound in the cell walls increased with the pH of the equilibrium solution (Fig. 5). Put^{2+} at 10 mN external concentration, however, was unable to displace protons from all of the uronic acids of the walls. Below pH 3.5, PAs were still present in the cell wall up to 12 to 25% of the CEC, depending on the valence and the concentration of the PA. This is clearly at variance with the behavior of mineral cations (Fig. 2; Van Cutsem and Gillet, 1983); below pH 2, the uronic acids of the cell wall should be protonated. This suggests that PA adsorption at very acidic pHs occurs by hydrogen bonding on some sterically accessible uronic acids. A similar observation was made on *N. flexilis* cell walls (not shown), suggesting that hydrogen bonding of PAs at such acidic pHs is a general feature of plant cell walls. However, such pHs are nonphysiological and are not expected to occur in vivo in the cell wall.

Quantitative Interpretation of the PA-H^+ Isotherms

Negatively charged uronates in the cell wall generate an electric field that interacts with two types of positive charges: protons and all other cations. A covalent link with a proton can reinstate a carboxylic function —COOH, whereas an electrostatic bond keeps cations in the vicinity of the polyanions. Protons and cations thus compete for the exchange sites of the walls. When a cell wall in equilibrium with a solution of cations is progressively acidified, two consecutive reactions occur: an exchange of cations for protons, followed by a protonation of carboxylates.

The first step can be written:

$$\frac{\overline{M^{z+}}}{z} + H^+ \Leftrightarrow \overline{H^+} + \frac{M^{z+}}{z}$$

and the equilibrium constant for one equivalent of exchanger is:

$$K_{ex} = \frac{\overline{C_H} \cdot C_M^{1/z}}{C_H \cdot \overline{C_M^{1/z}}}$$

where z is the valence of cation M, the bar indicating the adsorption in the polymer, $\overline{M^{z+}}/z$ is the concentration of the cation per unit charge in the adsorbed phase; C_M is the molar concentration of cation M in solution; C_H is the activity of the proton in solution; $\overline{C_H}$ is the activity of the proton in the adsorbed phase; and K_{ex} is the selectivity coefficient of the exchange reaction.

Once protons have entered the electrostatic field of the polyanions, they can protonate the uronates:

$$\overline{H^+} + \overline{A^-} \Leftrightarrow \overline{AH}$$

The equilibrium constant is expressed:

$$K_{HA} = \frac{\overline{C_{AH}}}{\overline{C_H} \cdot \overline{C_A}}$$

K_{HA} is the protonation constant of the carboxylates, $\overline{AH}$ is uronic acid, $\overline{A^-}$ is the corresponding anion, and $\overline{C_H}$ is the

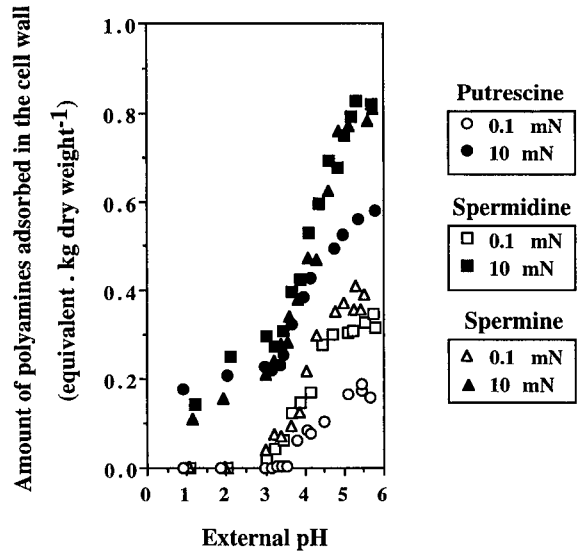

Figure 5. Influence of equilibrium solution pH on the amounts of Put^{2+}, Spd^{3+}, and Spm^{4+} adsorbed in carrot cell walls. Cell walls were equilibrated in 0.1 and 10 mN PA solutions.

proton activity in the adsorbed phase. The global exchange and protonation equation reads:

$$\frac{\overline{M^{z+}}}{z} + H^+ + \overline{A^-} \Leftrightarrow \overline{AH} + \frac{M^{z+}}{z}$$

$$K_{ex-HA} = \frac{\overline{C_{AH}}}{\overline{C_A}} \cdot \frac{C_M^{1/z}}{C_H \cdot \overline{C_M}^{1/z}}$$

The only value that is not experimentally accessible is $\overline{C_A} = \overline{C_H} + z\overline{C_M}$, the concentration of dissociated sites in the wall. It is approximated by $\overline{C_A} = z\overline{C_M}$, the number of equivalents of cation M adsorbed in the polymer. Considering that the electroselectivity favors the adsorption of multivalent cations, we implicitly assume that the proton concentration in the electric field close to charged sites is negligible compared with multivalent cation concentrations. Finally, the log form of the last equation can be formulated as a function of the degree of ionization $\alpha = \overline{C_A}/\overline{C_{At}}$, where $\overline{C_{At}} = \overline{C_A} + \overline{C_{AH}}$:

$$\log K_{ex-HA} = pH - \frac{1}{z}\log\frac{\overline{C_{At}}}{zC_M} - \log\frac{\alpha^{(z+1)/z}}{1-\alpha}$$

where $\log K_{ex-HA}$, the global equilibrium constant of exchange and protonation, is called apparent pK.

Interpretation of the PA-H^+ Isotherms

The nature of the interactions between PAs and uronates can be conjectured from the plot of the Log K_{ex-HA} of the PA-H^+ exchanges as a function of $\bar{N}_{A^-}$, the proportion of ionized exchange sites. The log K_{ex-HA} values of the 0.1 mN isotherms and up to 60% of the 10 mN isotherms have a relatively constant value of approximately 3.2, which is close to 3.36, the intrinsic ionization pKa of galacturonic acid (Fig. 6). This value is strikingly different from what is usually observed with cations such as Ca^{2+} or Cu^{2+} in *N. flexilis*, for example, for which the logarithmic coefficient is shifted 1.1 and 2.1 units down the pKa value, respectively (Van Cutsem and Gillet, 1983). This indicates the absence of selectivity other than electroselectivity between the two PAs and protons in the matrix phase.

In fact, PAs behave more ideally in the cell wall than does Ca^{2+}, for which additional stabilization arises from geometrical considerations. In other words, these isotherms indicate that PAs per se do not seem to induce any particularly favorable conformation of pectins such as egg boxes (Morris et al., 1982; Powell et al., 1982) that would lead to an increased selectivity of adsorption. This interpretation can be further substantiated by the results of ion-exchange isotherms involving three DAs differing only in the length of the aliphatic chains connecting the two amino groups.

Ca^{2+}-DAs Exchanges

The selectivity of the cell wall for the three DAs octanediamine, butanediamine (Put^{2+}), and ethanediamine was first studied by performing exchange isotherms against Ca^{2+}. The results (Fig. 7) show that (a) Ca^{2+} is

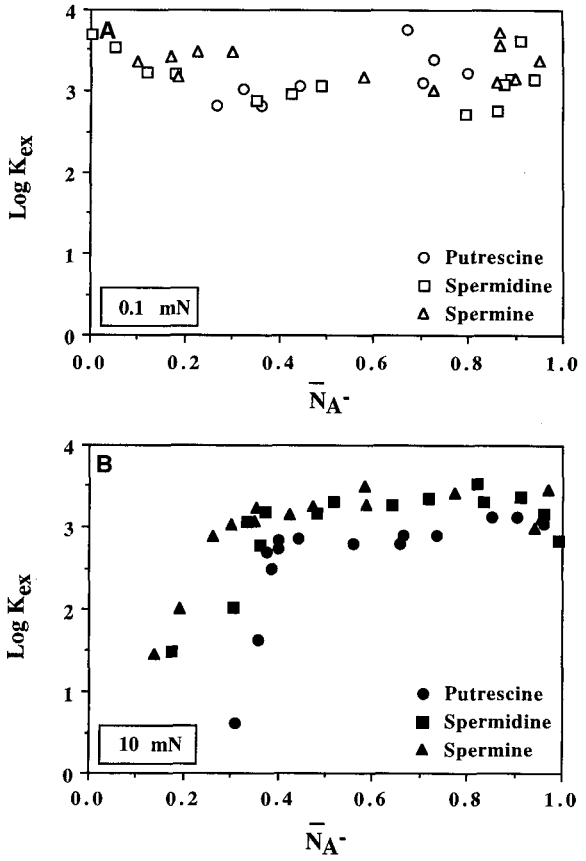

Figure 6. Evolution of the apparent pK_a (log K_{ex}) during deprotonation of the cell wall in the presence of 0.1 mN (A) and 10 mN (B) PA solutions. $\bar{N}_{A^-}$ is the ionization degree of the wall uronates.

preferred over most of the isotherms to any of the DAs, (b) the DAs behave differently according to their sizes, and (c) there is a range of pectic sites differing in their affinity for Ca^{2+}.

The Ca^{2+}-DO^{2+} isotherm shows a very strong selectivity for Ca^{2+} in preference to octanediamine. The interpretation of this result is straightforward: the distance between the two charged amino groups of DO^{2+} is much too large for the molecule to bind closely spaced uronates, whereas the shorter Put^{2+} and DE^{2+} have a behavior closer to the bivalent Ca^{2+} ion. The ln K_N coefficients of the three exchanges decrease monotonously, indicating that the last Ca^{2+} ions are far more difficult to displace from the wall pectins than the first ones. Obviously, PAs adsorb first on the pectic sites that have the lowest affinity for Ca^{2+}.

In fact, the wall CEC for DO^{2+} is only 0.25 equivalent kg^{-1} (31%) when the CEC for Put^{2+} and DE^{2+} reaches 0.6 (73%) and 0.72 (90%) equivalent kg^{-1}, respectively, meaning that in the absence of Ca^{2+} up to 70% of the uronic acids remain protonated at pH 5.5 when the sole counterion is octanediamine. The higher affinity pectic sites simply do not bind DO^{2+} but do bind to some extent the shorter Put^{2+} and especially DE^{2+}.

We can rule out accessibility problems in the wall matrix, since in its extended conformation, DO^{2+} is the same length as Spd^{3+} (Fig. 8). A simple explanation would be that oc-

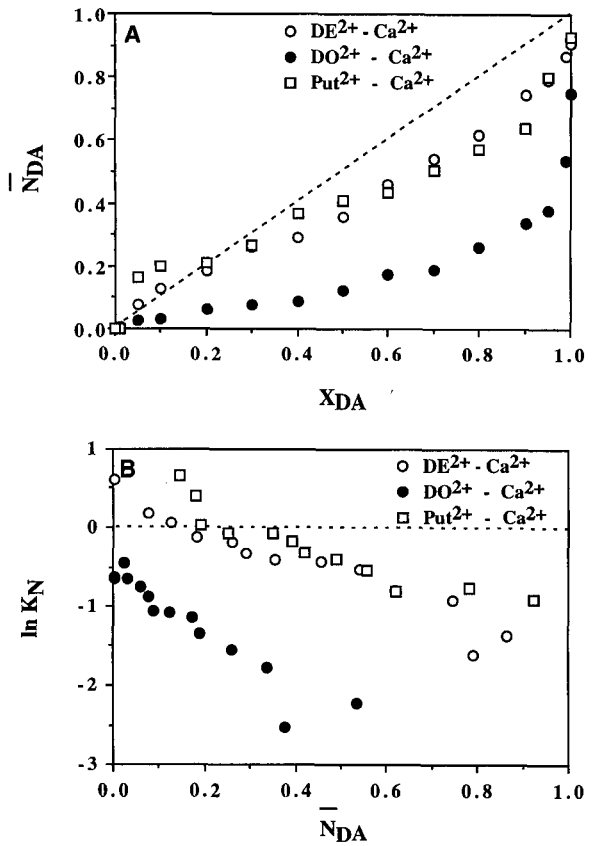

Figure 7. DA-Ca^{2+} ionic exchange isotherm. A, Equivalent fraction of the DA adsorbed in carrot cell walls ($\bar{N}_{DA}$) versus the equivalent fraction of the same DA (X_{DA}) present in the bathing solutions. B, Natural logarithm of the selectivity coefficient K_N versus the equivalent fraction of the DAs adsorbed in the cell wall ($\bar{N}_{DA}$).

tanediamine is sterically prevented from fitting within high-affinity sites, because its internal charge-to-charge distance is higher than for any of the studied PAs and much higher than the interuronate spacing within one or between two PGA chains. This picture can be refined with the help of triangular ion exchanges among the three PAs.

Triangular Exchanges among DAs

Three binary isotherms were carried out using 10 mN chloride solutions of DO^{2+}, Put^{2+}, and DE^{2+}. The results (Fig. 9) clearly show that the Put^{2+} versus DO^{2+} and the DO^{2+} versus DE^{2+} exchanges are nearly diagonal with the ln K_N values of the exchanges close to 0 (Fig. 9B). The fact that all of these ln K_N values are constant means that the wall uronic acids accessible to the two PAs adsorb them with an equal affinity. Since we know that the CEC for DO^{2+} is only about 31% of the total CEC, we can simply conclude once again that octanediamine occupies the lower affinity sites of the wall, whereas the higher-affinity sites are finally protonated in pure 10 mN DO^{2+} solutions and that these lower-affinity sites do not discriminate between PAs.

The selectivity of the last Put^{2+} versus DE^{2+} isotherm was not constant and revealed a selectivity reversal at about 50% of the exchange. As discussed above, the isotherms of these two shorter DAs versus Ca^{2+} were also closer to the diagonal than the one between Ca^{2+} and DO^{2+}. It appears that the DE^{2+} and Put^{2+} DAs distribute between two categories of exchange sites: low-affinity sites, where Put^{2+} adsorbs selectively, versus high-affinity sites, where DE^{2+} is preferred.

Since the only difference between the three DAs is the length of the C chain separating the amino groups, one possible hypothesis to explain the selectivity of these exchanges is that, because of its smaller size, DE^{2+} is more able than Put^{2+} to partially substitute for Ca^{2+} in keeping pectic molecules in close proximity. DE^{2+} thereby accesses more higher-affinity sites, whereas DO^{2+} suffers from steric hindrance and binds only "low-affinity uronates" (Fig. 10).

Biochemical Nature of Exchange Sites

It is now clear that the cell wall contains different types of exchange sites that discriminate among the surrounding cations for adsorption and exchange. These exchange sites differ first by their biochemical nature and environment: in carrot roots, only a marginal amount (<5% of the CEC) consists of glucuronic acid, but about 15% of the galacturonic acids belong to the hairy rhamnogalacturonan, which behaves very differently in the presence of ions compared with about 85% of PGA sequences (J.-F. Thibault, personal communication).

If we now turn to the geometry of PGA sequences, and stick to the well-known egg box model, we can distinguish between "high-affinity internal sites," i.e. uronates facing each other inside dimerized pectic chains, and "low-affinity external sites," i.e. galacturonates on the outside faces of the assembly that bind cations less strongly. We

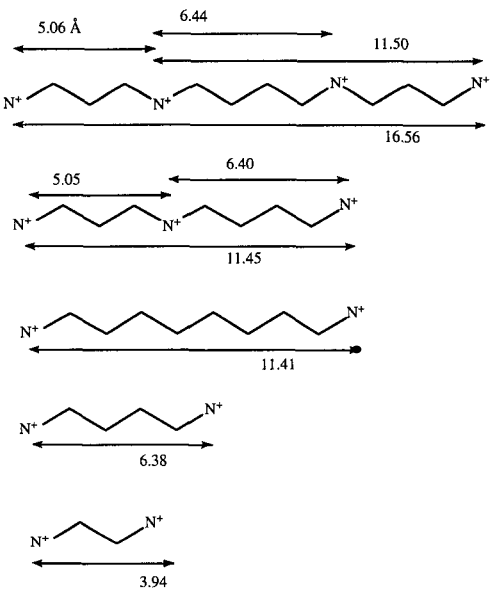

Figure 8. Inter-N distances of PAs. The main inter-N distances (Å) of the PAs studied are listed. From top to bottom: Spm^{4+}, Spd^{3+}, octanediamine, Put^{2+}, ethanediamine.

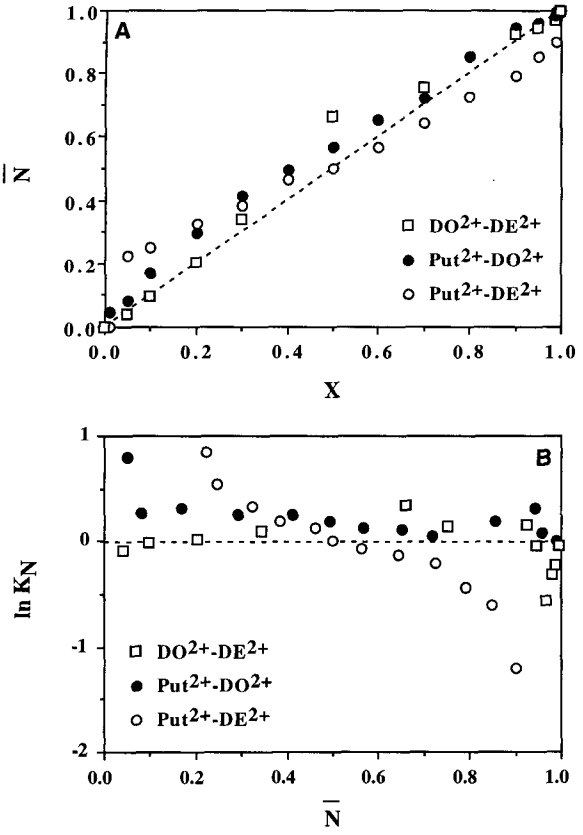

Figure 9. DA-DA ionic exchange isotherm. A, Equivalent fraction of DA adsorbed in the carrot cell walls ($\bar{N}$) versus the relative amount of the same DA (X) present in the bathing solutions. □, The equivalent fraction of DO^{2+} in the wall plotted as a function of its equivalent fraction in a binary DO^{2+}-DE^{2+} mixture; ●, Put^{2+} adsorbed in the wall plotted as a function of its equivalent fraction in a binary Put^{2+}-DO^{2+} mixture; ○, Put^{2+} adsorbed in the wall plotted as a function of its equivalent fraction in a binary Put^{2+}-DE^{2+} mixture. B, Natural logarithm of the selectivity coefficients K_N versus the equivalent fraction of the DAs adsorbed in the cell wall ($\bar{N}$).

hypothesize that, when a wall in its Ca^{2+} form is soaked in a solution that contains a short DA, the inner PGA sites keep their Ca^{2+} strongly, whereas rhamnogalacturonan I and outer PGA sites start losing Ca^{2+}. When the DA concentration is increased, the majority of the external sites and a growing proportion of the inner sites (but not all of them) fix the organic cation. The proportion of pectins that protonate instead depends on PA valence, geometry, and concentration.

If we now restrict the discussion to the naturally available PAs, we conclude that, at the lower than millimolar concentrations reported in the literature and in the presence of Ca^{2+} cations, Put^{2+} adsorption in the wall will be restricted to the lower-affinity sites, i.e. rhamnogalacturonan I and the outer sites of dimerized PGA chains. On the other hand, the higher charged Spd^{3+} and Spm^{4+} compete more efficiently with Ca^{2+} and access all of the exchange sites. We can thus expect the two latter PAs to react differently on the pectic fraction of the wall compared with Put^{2+}.

Biological Implications

It is interesting that the two groups of PAs (Put^{2+}, which does not access the high-affinity sites, versus Spd^{3+} and Spm^{4+}, which do access them) seem to act differentially in several biological systems. For example, the extra Put^{2+} synthesized in the leaves of *Sinapis alba* induced to flower after a long day is a necessary component of the floral stimulus (Havelange et al., 1996). The level of free Put^{2+} in submerged shoots of *Scirpus mucronatus* increases and is coincident with the increase in shoot length, whereas Spd^{3+} and Spm^{4+} contents decrease (Lee et al., 1996). *D. carota* cells transformed with a mouse Orn decarboxylase cDNA under the control of a cauliflower mosaic virus 35S promoter show a significant increase in the cellular content of Put^{2+}, but Spd^{3+} remains unaffected. These transformed cells exhibit improved somatic embryogenesis in auxin-free medium (Bastola and Minocha, 1995).

It is tempting to suggest that some of the numerous physiological effects of PAs could be mediated by their differential ionic interaction with pectic fragments that are known to act on morphogenesis and pathogenesis in plants (Van Cutsem and Messiaen, 1994). We are therefore currently studying the effect of PAs on the conformation and signaling properties of oligopectates in carrot cell suspensions.

CONCLUSIONS

The different exchange isotherms presented in this paper showed a concentration- and pH-dependent adsorption of the PAs on the uronates of the carrot cell walls. The ionic selectivity sequence was $Spm^{4+} > Spd^{3+} \approx Ca^{2+} > Put^{2+} \approx DE > DO$. This selectivity sequence can be partly ex-

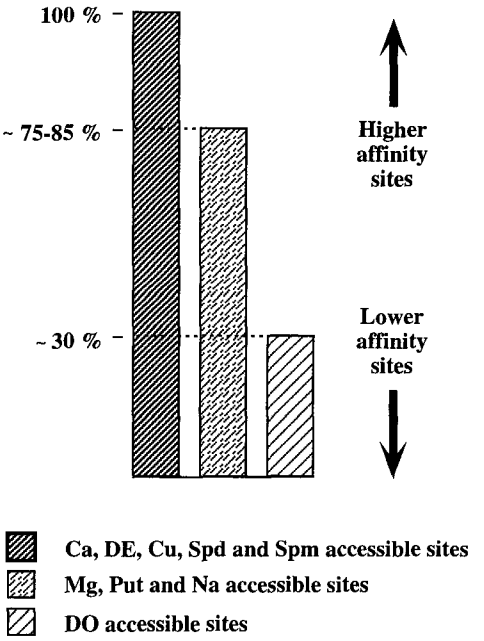

Figure 10. Diagrammatic representation of the accessibility of the carrot cell wall uronates to the different inorganic cations, DAs and PAs.

plained by the valence and the geometry of the PAs and the inability of DAs to adsorb on all of the uronates of the wall, and partly by the heterogeneity of the exchange sites that distribute between high- and low-affinity sites.

ACKNOWLEDGMENTS

We thank Dr. J. Wouters for help with the computer simulation of PAs and Nathalie Constant for preliminary work.

Received August 5, 1996; accepted October 27, 1996.

LITERATURE CITED

Angelini R, Bragaloni M, Federico R, Infantino A, Porta-Puglia A (1993) Involvement of polyamines, diamine oxidase and peroxidase in resistances of chickpea to *Ascochyta rabiei*. J Plant Physiol **142:** 704–709

Apelbaum A, Camellakis ZN, Applewhite PB, Kaur-Sawhney R, Galston AW (1988) Binding of spermidine to a unique protein in thin-layer tobacco tissue culture. Plant Physiol **88:** 996–998

Bastola RD, Minocha SC (1995) Increased putrescine biosynthesis through transfer of mouse ornithine decarboxylase cDNA in carrot promotes somatic embryogenesis. Plant Physiol **109:** 63–71

Basu HS, Schwietert HCA, Feuerstein BG, Marton LJ (1990) Effect of variation in the structure of spermine on the association with DNA and the induction of DNA conformational changes. Biochem J **269:** 329–334

Charnay D, Nari J, Noat G (1992) Regulation of plant cell wall pectin methyl esterase by polyamines—interaction with the effect of metal ions. Eur J Biochem **205:** 711–714

D'Orazi D, Bagni N (1987) In vitro interactions between polyamines and pectic substances. Biochem Biophys Res Commun **148:** 1159–1163

Egea-Cortines M, Mizrahi Y (1991) Polyamines in cell division, fruit set and development, and seed germination. *In* RD Slocum, HE Flores, eds, Biochemistry and Physiology of Polyamines in Plants. CRC, Boca Raton, FL, pp 143–158

Havelange A, Lejeune P, Bernier G, Kaur-Sawhney R, Galston AW (1996) Putrescine export from leaves in relation to floral transition in *Sinapis alba*. Physiol Plant **96:** 59–65

Lee T-M, Shieh Y-J, Chou C-H (1996) Role of putrescine in enhancing shoot elongation in *Scirpus mucronatus* under submergence. Physiol Plant **96:** 419–424

Maple JR, Dinur U, Hagler AT (1988) Derivation of force fields for molecular mechanics and dynamics from ab initio energy surfaces. Proc Natl Acad Sci USA **85:** 5350–5354

Maple JR, Hwang M-L, Stockfish TP, Dinur U, Waldman M, Ewig CS, Hagler AT (1984) Derivation of class II force fields. Methodology and quantum force field for the alkyl functional group and alkane molecules. J Comput Chem **15:** 162–182

Mariani P, D'Orazi D, Bagni N (1989) Polyamines in primary walls of carrot cells; endogenous content and interactions. J Plant Physiol **135:** 508–510

Mehta HS, Saftner RA, Mehta RA, Davies PJ (1994) Identification of posttranscriptionally modified 18-kilodalton protein from rice as eukaryotic translocation initiation factor 5A. Plant Physiol **106:** 1413–1419

Montague M, Armstrong T, Jaworski E (1979) Polyamine metabolism in embryogenic cells of *Daucus carota*. II. Changes in arginine decarboxylase activity. Plant Physiol **63:** 341–345

Morris ER, Powell DA, Gidley MJ, Rees DA (1982) Conformation and interactions of pectins. I. Polymorphism between gel and solid states of calcium polygalacturonate. J Mol Biol **155:** 507–516

Moustacas A-M, Nari J, Borel M, Noat G, Ricard J (1991) Pectin methylesterase, metal ions and plant cell-wall expansion. Biochem J **279:** 351–354

Murashige T, Skoog F (1962) A revised medium for rapid growth and bioassays with tobacco tissue cultures. Physiol Plant **15:** 473–497

Powell DA, Morris ER, Gidley MJ, Rees DA (1982) Conformation and interactions of pectins. II. Influence of residue sequence on chain association in calcium pectate gels. J Mol Biol **155:** 517–531

Schuber F, Hong K, Düzgünes N, Papahadjopoulos D (1983) Polyamines as regulators of membrane fusion: aggregation and fusion of liposomes. Biochemistry **22:** 6134–6140

Tassoni A, Antognoni F, Bagni N (1996) Polyamine binding to plasma membrane vesicles from zucchini hypocotyls. Plant Physiol **110:** 817–824

Van Cutsem P, Gillet C (1981) A thermodynamic study of the Cu^{2+}-Zn^{2+} ion exchange in the *Nitella flexilis* cell wall. Plant Soil **62:** 367–375

Van Cutsem P, Gillet C (1982) Activity coefficients and selectivity values of Cu^{++}, Zn^{++} and Ca^{++} ions adsorbed in the *Nitella flexilis* L. cell wall during triangular ion exchanges. J Exp Bot **33:** 847–853

Van Cutsem P, Gillet C (1983) Proton-metal cation exchange in the cell wall of *Nitella flexilis*. Plant Physiol **73:** 865–867

Van Cutsem P, Messiaen J (1994) Biological effects of pectic fragments in plant cells. Acta Bot Neerl **43:** 231–245

Ye XS, Avdiushko SA, Kuc J (1994) Effect of polyamines on in vitro phosphorylation of soluble and plasma membrane proteins in tobacco, cucumber and *Arabidopsis thaliana*. Plant Sci **97:** 109–118

York WS, Darvill AG, McNeil M (1986) Isolation and characterization of plant cell walls and cell wall components. Methods Enzymol **118:** 3–40

York WS, Darvill AG, McNeil M, Stevenson TT, Albersheim P (1985) Isolation and characterization of plant cell walls and cell wall components. Methods Enzymol **118:** 3–40